Structural Basis for the Inhibition of the LSD1 Histone Demethylase by the Antidepressant *trans*-2-Phenylcyclopropylamine[†,‡]

Maojun Yang,[§] Jeffrey C. Culhane,[||] Lawrence M. Szewczuk,[||] Pegah Jalili,[⊥] Haydn L. Ball,[⊥] Mischa Machius,[#] Philip A. Cole,[||] and Hongtao Yu*[,§]

Departments of Pharmacology, Internal Medicine, and Biochemistry, The University of Texas Southwestern Medical Center, 6001 Forest Park Road, Dallas, Texas 75390, and Department of Pharmacology and Molecular Sciences, The Johns Hopkins University School of Medicine, Baltimore, Maryland 21205

Received April 9, 2007; Revised Manuscript Received May 5, 2007

ABSTRACT: Histone modifications, such as acetylation and methylation, are important epigenetic marks that regulate diverse biological processes that use chromatin as the template, including transcription. Dysregulation of histone acetylation and methylation leads to the silencing of tumor suppressor genes and contributes to cancer progression. Inhibitors of enzymes that catalyze the addition and removal of these epigenetic marks thus have therapeutic potential for treating cancer. Lysine-specific demethylase 1 (LSD1) is the first discovered histone lysine demethylase and, with the help of its cofactor CoREST, specifically demethylates mono- and dimethylated histone H3 lysine 4 (H3−K4), thus repressing transcription. Because LSD1 belongs to the family of flavin adenine dinucleotide (FAD)-dependent amine oxidases, certain inhibitors of monoamine oxidases (MAOs), including the clinically used antidepressant *trans*-2-phenylcyclopropylamine (PCPA; tranylcypromine; Parnate), are also capable of inhibiting LSD1. In this study, we have further measured the kinetic parameters of the inhibition of LSD1 by PCPA and determined the crystal structure of LSD1−CoREST in the presence of PCPA. Our structural and mass spectrometry analyses are consistent with PCPA forming a covalent adduct with FAD in LSD1 that is distinct from the FAD−PCPA adduct of MAO B. The structure also reveals that the phenyl ring of the FAD−PCPA adduct in LSD1 does not form extensive interactions with active-site residues. This study thus provides the basis for designing more potent inhibitors of LSD1 that contain substitutions on the phenyl ring of PCPA to fully engage neighboring residues.

Post-translational modifications of histones, including acetylation, phosphorylation, methylation, ubiquitination, and sumoylation, regulate gene transcription and other chromatin-templated processes by directly changing the chromatin structure and/or through recruitment of effectors containing protein modules that bind selectively to modified histones (*1*, *2*). Histone lysine methylation can either activate or repress transcription, depending upon the site and degree (mono-, di-, and trimethylation) of modifications (*3*, *4*). Because the half-life of methylated histones is longer than that of bulk histones, histone methylation has been thought of as an irreversible epigenetic mark (*5*). The recent discoveries of two classes of histone lysine demethylases have changed this view (*5*). Lysine-specific demethylase 1 (LSD1;[1] also known as BHC110 and AOF2) was the first histone lysine demethylase discovered and specifically demethylates mono- and dimethylated histone H3 lysine 4 (H3−K4) (*6*). The catalytic domain of LSD1 shares significant sequence and structural similarity with amine oxidases and removes methyl groups through a flavin adenine dinucleotide (FAD)-dependent amine oxidation reaction (*6*, *7*). Because of the requirement for the presence of a lone pair of electrons in the unprotonated state of Nϵ of the methylated lysine, LSD1 cannot demethylate trimethylated lysine residues. Therefore, similar to other histone modifications, histone methylation is a dynamic process and regulated by enzymes with opposing activities.

Dimethylated H3−K4 is enriched in the promoter regions of actively transcribed genes (*4*). Consistently, LSD1 is a component of various transcriptional corepressor complexes that often include histone deacetylases 1/2 (HDAC1/2) and CoREST (*8*−*11*). Although LSD1 alone is capable of demethylating H3−K4 in peptide or bulk histone substrates, demethylation of H3−K4 in nucleosomes by LSD1 requires CoREST (*12*, *13*). We have recently determined the crystal

[†] This work is supported in part by the National Institutes of Health (to P.A.C.), the W. M. Keck Foundation (to H.Y.), and the Welch Foundation (to H.Y.).

[‡] Coordinates and structure factors have been deposited in the Protein Data Bank under accession code 2UXX.

* To whom correspondence should be addressed. Telephone: (214) 645-6161. Fax: (214) 645-6156. E-mail: hongtao.yu@utsouthwestern.edu.

[§] Department of Pharmacology, The University of Texas Southwestern Medical Center.

[||] The Johns Hopkins University School of Medicine.

[⊥] Department of Internal Medicine, The University of Texas Southwestern Medical Center.

[#] Department of Biochemistry, The University of Texas Southwestern Medical Center.

[1] Abbreviations: LSD1, lysine-specific demethylase 1; H3−K4, histone H3 lysine 4; FAD, flavin adenine dinucleotide; HDAC, histone deacetylase; MAO, monoamine oxidase; PCPA, *trans*-2-phenylcyclopropylamine; CPG, *N*-(cyclopropyl)glycine; MSOX, monomeric sarcosine oxidase.

10.1021/bi700664y CCC: $37.00
Published on Web 06/15/2007

structure of the LSD1−CoREST complex and showed that CoREST stimulates nucleosomal demethylation by LSD1 through DNA binding by its SANT2 domain (*14*). The LSD1−CoREST-containing transcriptional corepressor complexes are recruited to specific promoters by sequence-specific DNA-binding proteins. For example, through its interaction with CoREST, the transcriptional repressor, REST (RE1 silencing transcription factor/neural-restrictive silencing factor), recruits LSD1−CoREST to promoters of neuronal-specific genes, thus blocking their expression in non-neuronal tissues in vertebrates (*6*, *13*).

Global epigenetic alterations, including changes in histone acetylation and methylation, can lead to the silencing of key tumor suppressor genes and collaborate with genetic mutations to promote tumorigenesis (*15*). HDAC inhibitors indeed have antitumor activities (*16*), presumably through reactivating the expression of tumor suppressors. Given the frequent physical association of LSD1 with HDACs and the positive cooperativity between LSD1 and HDACs in modifying chromatin (*17*), it is very likely that LSD1 and HDACs collaborate to repress the transcription of common sets of genes. Thus, chemical inhibitors of LSD1 may exhibit antitumor activities on their own and/or have synergistic effects with HDAC inhibitors.

LSD1 belongs to the superfamily of FAD-containing amine oxidases. Monoamine oxidases (MAO A and B) are responsible for the oxidative deamination of neurotransmitters, including serotonin and dopamine (*18*). Small molecules containing cyclopropylamine or propargylamine moieties are irreversible inhibitors of MAOs that covalently modify the FAD cofactor. One such inhibitor, *trans*-2-phenylcyclopropylamine (referred to as PCPA hereafter; also known as tranylcypromine and Parnate), is used clinically as an antidepressant. We have shown that histone H3 peptides containing propargyl-derivatized K4 are potent, mechanism-based suicide inactivators of LSD1 (*19*, *20*), suggesting that LSD1 and MAOs use similar mechanisms for catalysis. Interestingly, two recent studies showed that PCPA efficiently inhibited LSD1, albeit with reduced potency as compared to its inhibition of MAOs (*21*, *22*). In this study, we have performed kinetic, UV/vis spectroscopy, and mass spectrometry analyses of the inhibition of LSD1 by PCPA. We have determined the crystal structure of the LSD1−CoREST complex treated with PCPA. Our results show that PCPA covalently modifies the FAD cofactor of LSD1 and suggest that the FAD−PCPA adduct is distinct from that in MAO B. Our structure serves as a valuable starting point for the design of more potent LSD1 inhibitors.

MATERIALS AND METHODS

Protein Expression and Purification. The complex of LSD1ΔN (171−852)−CoREST-C (286−482) was purified as described (*14*). Briefly, both proteins were expressed in *Escherichia coli* as glutathione *S*-transferase (GST) fusion and N-terminal His_6-tagged proteins, respectively. GST−LSD1ΔN was purified from bacterial lysates by glutathione-sepharose resin and used in demethylation assays. For protein crystallization, following protease digestion to remove GST on beads, LSD1ΔN was mixed with CoREST-C that was purified using Ni^{2+}-affinity chromatography. The resulting LSD1ΔN−CoREST-C complex (referred to as LSD1−CoREST for simplicity) was purified by gel-filtration chromatography and concentrated to about 10 mg/mL in a buffer containing 25 mM *N*-2-hydroxyethylpiperazine-*N*′-2-ethanesulfonic acid (HEPES) at pH 7.4, 200 mM NaCl, 1 mM PMSF, and 5 mM dithiothreitol (DTT). For kinetic studies, GST−LSD1 was prepared as described with 1 mM β-mercaptoethanol in the stock solution (*20*).

Crystallization, Data Collection, and Structure Determination. PCPA was added to the purified LSD1−CoREST complex at a final concentration of 1.0 mM. After incubation on ice for 30 min, the protein was used to set up crystallization trials with the vapor diffusion method using a reservoir solution consisting of 0.8 M lithium sulfate, 0.8 M ammonium sulfate, 0.4 M sodium chloride, 0.1 M sodium citrate at pH 5.6, and 10 mM DTT. Crystals emerged overnight and matured in about 1 week. The crystals were incubated with the reservoir solution supplemented with 23% (v/v) glycerol and 1.0 mM PCPA and then flash-cooled in liquid propane. Diffraction data were collected at beamline 19-ID (SBC-CAT) at the Advanced Photon Source (Argonne National Laboratory, Argonne, IL) and processed with HKL2000 (*23*). The PCPA-modified LSD1−CoREST crystals showed significant anisotropy, with diffraction to a Bragg spacing (d_{min}) of about 2.75 Å along the *b* and *c* axes but only to about 3.2 Å along the *a* axis, resulting in somewhat lower completeness at the high-resolution limit. Crystals exhibited the symmetry of space group *I*222, with cell dimensions of $a = 121$ Å, $b = 179$ Å, $c = 236$ Å, and contained one complex per asymmetric unit and 82% solvent.

The structure of LSD1−CoREST−PCPA was determined by difference Fourier methods using the structure of the LSD1−CoREST complex [Protein Data Bank (PDB) 2IW5] as a starting model with water molecules and the FAD cofactor removed. Refinement was carried out with REFMAC5 (*24*) from the CCP4 package (*25*) with a random 1529 reflections set aside for the R_{free} calculation, interspersed with manual rebuilding using Coot (*26*). After the protein part was complete, the electron density clearly showed that the FAD cofactor was covalently modified. The resolution of the electron density was not high enough to allow for unambiguous assignment of the chemical structure of the FAD−PCPA adduct. We therefore modeled the FAD−PCPA adduct based on reaction mechanisms, mass spectrometry, and UV/vis spectroscopy data. For structure refinement, data between a d_{min} of 49.0 and 2.75 Å were used, resulting in an R_{work} of 23.7% and an R_{free} of 25.8% (Table 1). The average *B* value for the refined model is 97.5 $Å^2$. The final model contains residues 171−835 of LSD1 and residues 307−442 of CoREST, the FAD−PCPA adduct, and two water molecules.

Steady-State Inactivation Assay of LSD1 by PCPA. Inhibition of LSD1 by PCPA was monitored using the peroxidase-coupled assay system as described (*27*). Briefly, the 150 μL reactions were initiated by adding 50 μL of buffered peptide substrate (60 μM diMeK4H3-21 = K_m) and PCPA at varying concentrations (0, 62.5, 125, 250, 500, and 1000 μM) simultaneously to reactions mixtures (100 μL) consisting of 50 mM HEPES at pH 7.5, 0.1 mM 4-aminoantipyrine, 1 mM 3,5-dichloro-2-hydroxybenzenesulfonic acid, 0.76 μM horseradish peroxidase (Worthington Biochemical Corporation), and 7.5 μg (480 nM) LSD1 at a temperature of 25 °C. Progress curves obtained in the presence of PCPA were fit

Table 1: Data Collection, Structure Determination, and Refinement[a]

data collection	
space group	*I*222
cell parameters: *a*, *b*, *c* (Å)	120.8, 178.5, 235.9
resolution range (Å)	49.20−2.75 (2.78−2.75)
unique reflections	65 220 (1742)
multiplicity	12.2 (5.3)
data completeness (%)	98.0 (80.9)
R_{merge} (%)[b]	6.5 (62.3)
$I/\sigma(I)$	42.0 (2.0)
Wilson *B* value (Å^2)	84.9
refinement statistics	
resolution range (Å)	49.00−2.75
number of reflections R_{work}/R_{free}	63 643/1529
atoms (non-H protein, inhibitor)	6309
water molecules	2
FAD/PCPA	63
R_{work}/R_{free} (%)	23.62/25.80
rmsd bond length (Å)	0.06
rmsd bond angle (deg)	1.073
cross-validated σ_A-coordinate error (Å)	0.20
mean *B* value (Å^2)	97.5
rms *B* value (Å^2) main chain/side chain	0.341/0.537
correlation coefficient F_o-F_c work/free	0.940/0.925
missing residues	LSD1Δ*N*: 836−852 CoREST-C: 284−307, 443−482

[a] Data for the outermost shell are given in parentheses. [b] $R_{merge} = 100\sum_h\sum_i|I_{h,i} - \langle I_h\rangle|/\sum_h\sum_i I_{h,i}$, where the outer sum (*h*) is over the unique reflections and the inner sum (*i*) is over the set of independent observations of each unique reflection.

to the following single exponential for slow-binding inhibitors, which assumes a steady-state velocity of 0 (*28*):

$$\text{product} = v_0(1 - e^{-kt})/k + \text{offset} \quad (1)$$

The k_{obs} values were then analyzed by the method of Kitz and Wilson to yield k_{inact} and $K_{i(inact)app}$. The following equation was used to extract kinetic constants from the Kitz−Wilson analysis (*29*):

$$k_{obs} = (k_{inact}[I])/(K_{i(inact)app} + [I]) \quad (2)$$

$K_{i(inact)app}$ was extrapolated to 0 substrate to yield $K_{i(inact)}$ by:

$$K_{i(inact)app} = K_{i(inact)}(1 + S/K_m) \quad (3)$$

The $t_{1/2}$ for inactivation at saturation was obtained from eq 4:

$$t_{1/2} = (\ln 2)/k_{inact} \quad (4)$$

UV/Vis Spectroscopy Analysis of the Inactivation of LSD1 by PCPA. GST−LSD1 (10 μM) was either treated or not treated with 500 μM PCPA for 60 min at 25 °C in 50 mM HEPES (pH 7.5). The samples were then cleared by centrifugation at 14000*g* for 10 min, and UV/vis spectra were recorded between 300 and 600 nm. For time-dependent spectral analysis, GST−LSD1 (1.5 μM) was treated with 500 μM PCPA at 25 °C in 50 mM HEPES at pH 7.5 and the decrease in absorbance at 468 nm was monitored every 1.2 s for 10 min. Reactions were initiated by the addition of buffered PCPA. The k_{obs} value was extracted by fitting the data to eq 1. Reactions were carried out in triplicates.

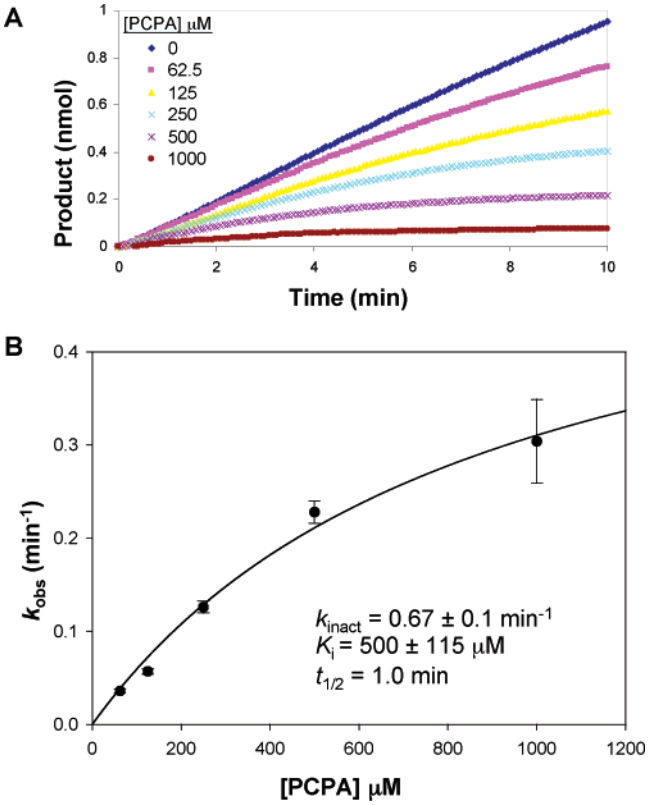

FIGURE 1: Time- and concentration-dependent inactivation of LSD1 by PCPA. (A) Steady-state progress curves obtained for the inactivation of LSD1 by 0, 62.5, 125, 250, 500, and 1000 μM PCPA using the peroxidase-coupled assay system. Experiments were carried out in duplicate. (B) Rate constants (k_{obs}) for the time-dependent inactivation of LSD1 by PCPA were extracted from steady-state data by single-exponential fits and analyzed by the method of Kitz and Wilson (*29*).

Analysis of the FAD−PCPA Conjugate by MALDI−TOF Mass Spectrometry. GST−LSD1 (10 μM) was treated with 500 μM tranylcypromine overnight at 25 °C in 50 mM HEPES (pH 7.5). The sample was then denatured with 4 M guanidinium hydrochloride plus 0.1% trifluoroacetic acid (TFA), applied to a C_{18} ZipTip (Millipore) column, and eluted with 75:25 CH_3CN/H_2O containing 0.05% TFA. The eluent was analyzed by MALDI−TOF mass spectrometry in α-cyano-4-hydroxycinnamic acid.

RESULTS AND DISCUSSION

Kinetic Analysis of Inhibition of LSD1 by PCPA. Previous studies have shown that PCPA inhibited LSD1 with an IC_{50} of 2 μM, whereas it inhibited MAOs with an IC_{50} of about 20 μM (*21*). It was thus suggested that PCPA was a more potent inhibitor of LSD1, as compared to MAOs. This finding further raised the provocative possibility that LSD1 was a relevant target for the efficacy of PCPA in the treatment of depression. However, that study used bulk histones and nucleosomes as the substrates for LSD1 and used qualitative Western blotting to monitor the activity of LSD1 (*21*). Furthermore, because PCPA is an irreversible covalent inhibitor of LSD1 and MAO, comparisons of the IC_{50} values might be misleading. We thus performed kinetic analysis of the inhibition of GST−LSD1 by PCPA using a dimethyl K4-containing H3 peptide (diMeK4H3-21) as the substrate in a well-established quantitative demethylase assay (*27*). Our analysis revealed that PCPA inhibited GST−LSD1

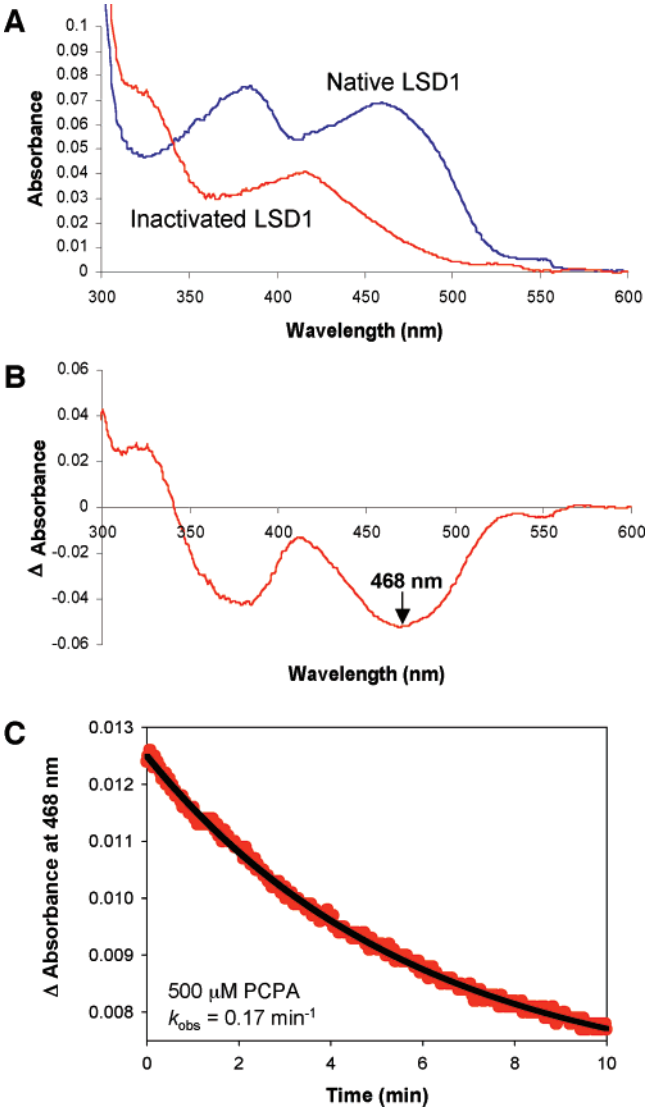

FIGURE 2: UV/vis spectroscopy analysis of the inactivation of LSD1 by PCPA. (A) UV/vis spectra of native and PCPA-inactivated LSD1. (B) Difference spectrum generated by subtracting the absorbance spectrum of native LSD1 from the absorbance spectrum of PCPA-inactivated LSD1. The plot indicates that the maximum change occurs at 468 nm. (C) Time-dependent spectral changes at 468 nm of GST−LSD1 (1.5 μM) treated with PCPA (500 μM).

in a time- and concentration-dependent manner, consistent with irreversible covalent inhibition of LSD1 by PCPA (Figure 1). The $K_{i(inact)}$ and k_{inact} for the inhibition of GST−LSD1 by PCPA were 500 ± 115 μM and 0.67 ± 0.1 min^{-1}, respectively. In this system, GST−LSD1 displayed a k_{cat} of 3.1 ± 0.1 min^{-1} and a K_m of 50 ± 5 μM for diMeK4H3-21. The k_{cat}/k_{inact} ratio was thus 4.6, indicating that inactivation of LSD1 by PCPA occurred with similar rates as the demethylation of substrates, consistent with PCPA being a mechanism-based suicide inactivator of LSD1. During the course of our studies, Schmidt and McCafferty reported a kinetic analysis of the inhibition of LSD1 and MAO A and B enzymes by PCPA (*22*). The kinetic parameters of inhibition of LSD1 reported here were largely in agreement with those reported by Schmidt and McCafferty (*22*). In their study, McCafferty and co-workers demonstrated that PCPA was a more potent inhibitor for MAO B than for LSD1 (*22*). However, it remains possible that high doses of PCPA may inhibit LSD1 in addition to MAO A and B and contribute

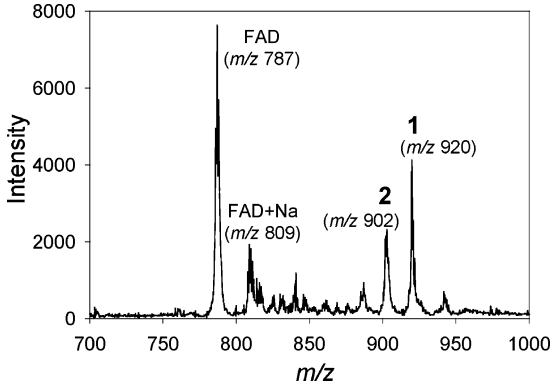

FIGURE 3: MALDI−TOF analysis of the FAD−PCPA conjugate. (A) MALDI−TOF spectrum showing the presence of two conjugate species (**1** and **2** in Scheme 1) as well as a free FAD cofactor. The FAD−PCPA adduct is proposed to exist in equilibrium between its hydrated (**1**) and dehydrated (**2**) forms.

to either the efficacy or the side effects of PCPA as an antidepressant.

UV/Vis Spectroscopy Analysis of the Inhibition of LSD1 by PCPA. We next analyzed the inhibition of LSD1 by PCPA using absorbance spectroscopy. In the absence of PCPA, FAD had a characteristic absorbance spectrum with two peaks between 350 and 500 nm (Figure 2A). The addition of PCPA dramatically altered the absorbance spectrum of FAD, with a single maximum at around 415 nm (Figure 2A), indicating covalent modification of FAD by PCPA. We also examined the kinetics of the formation of the FAD−PCPA adduct by monitoring absorbance changes at 468 nm (Figure 2B). The data were fitted to a pseudo-first-order process with an apparent rate constant of 0.17 min^{-1} (Figure 2C). This rate was similar to the k_{inact} of PCPA, suggesting that the formation of this adduct was a major process accounting for LSD1 inactivation by PCPA. Because PCPA is optically active and high concentrations of PCPA are expected to interfere with the optical assay, we did not perform the optical spectroscopy with PCPA at saturating concentrations to accurately determine k_{inact}.

Proposed Structure and Mechanism of Formation of the FAD−PCPA Adduct. Covalent inhibitors of FAD-dependent amine oxidases have been shown to modify either N(5) or C(4a) atoms of FAD (*30*). We have recently shown that a propargyl-K4-derivatized H3 peptide inhibitor of LSD1 (propargylK4H3-21) covalently attached to FAD N(5) (*20*). The absorbance spectrum of PCPA-modified FAD in LSD1 was very different from that of FAD modified by propargylK4H3-21 (*20*) but was very similar to that of *N*-(cyclopropyl)glycine (CPG)-modified FAD in monomeric sarcosine oxidase (MSOX) (*31*). The chemical structure of CPG-modified FAD in MSOX has been determined by X-ray crystallography to high resolution and contains a five-membered ring connecting N(5) and C(4a) of FAD (*31*). A single-electron-transfer mechanism has been proposed for the formation of this adduct (*31*). Because MSOX and LSD1 are likely to use similar mechanisms for catalysis and because the FAD−PCPA adduct in LSD1 has a very similar absorbance spectrum as the FAD−CPG adduct in MSOX, PCPA is likely to inactivate LSD1 through a similar single-electron-transfer mechanism (Scheme 1). In this scheme, FAD first extracts an electron from the nitrogen of PCPA, forming a cation radical. In pathway **a**, facile opening of the cyclo-

Scheme 1

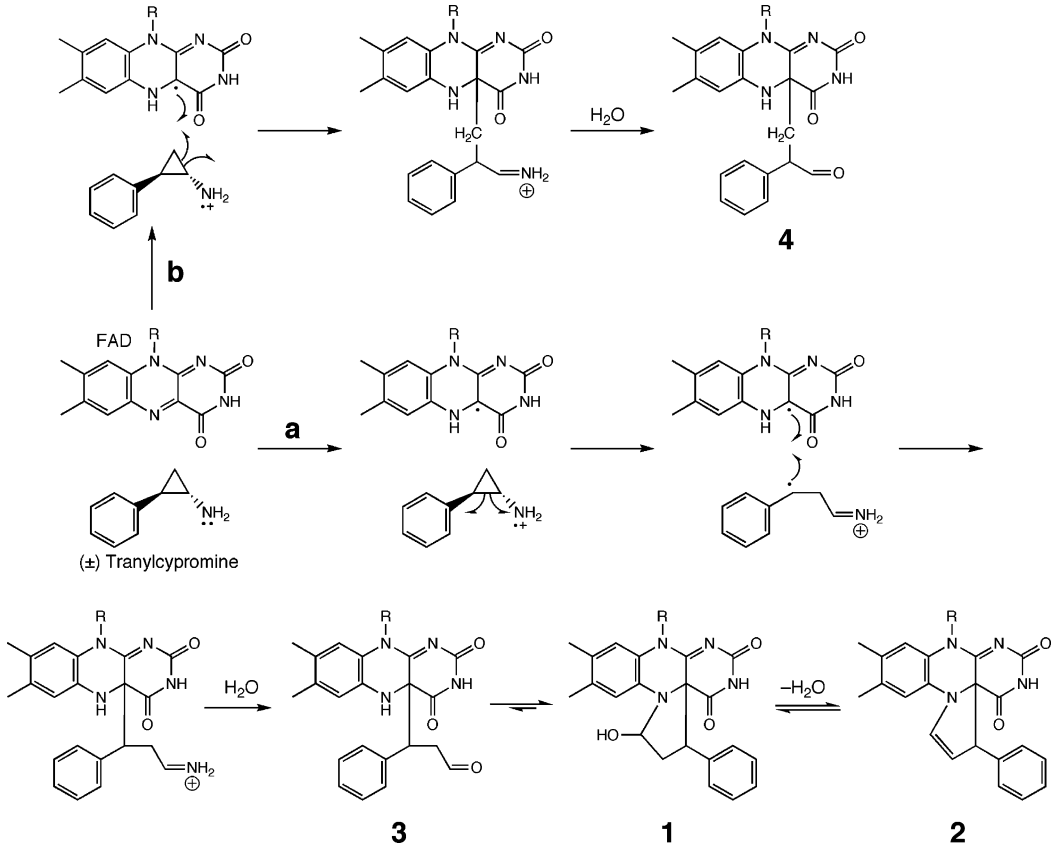

propyl ring leads to the formation of a benzylic carbon radical and an imine intermediate. The reaction of this benzylic radical of PCPA with C(4a) of FAD followed by hydrolysis of the imine would yield compound **3**. Compound **3** would be expected to undergo cyclization to produce compound **1** containing a five-membered ring linking C(4a) and N(5) of FAD. In pathway **b**, an alternative route of cyclopropyl ring opening results in the formation of an extremely unstable primary carbon radical, which is energetically unfavorable. However, the ring-opening reaction and the bond formation between FAD and PCPA can occur in a concerted fashion, which ultimately produces compound **4**. Indeed, compound **4** is the major adduct formed during the inactivation of MAO B by PCPA (*30*).

Mass Spectrometry Analysis of the FAD−PCPA Adduct. Because FAD is not covalently attached to LSD1, we were able to isolate the FAD−PCPA adduct by high-performance liquid chromatography (HPLC) and analyze it by MALDI−TOF mass spectrometry. We observed two major peaks in the mass spectrum of FAD species isolated from PCPA-inactivated LSD1: a peak at 787 Da corresponding to the expected mass of free FAD and a second peak at 920 Da that matched the expected mass of both compounds **1** and **4** (Figure 3A). Compound **4** has been suggested to be the FAD−PCPA adduct in LSD1 by McCafferty and co-workers (*22*). However, we also observed a significant minor peak at 902 Da, 18 Da less than the mass of **1** and **4** (Figure 3A). As shown in Scheme 1, dehydration of compound **1** produces compound **2** that has an expected mass of 902 Da. Thus, the formation of **2** implicates compound **1** as the FAD−PCPA adduct in LSD1. In contrast, the formation of FAD species with a mass of 902 Da is not readily explained by adduct formation affording compound **4**. Moreover, we noticed that the FAD−PCPA adduct was heat-unstable. Indeed, mass spectrometry analysis confirmed that FAD species isolated from PCPA-inactivated LSD1 after heat denaturation contained mostly free FAD (data not shown). The FAD species with a mass of 902 Da was also observed, indicating the formation of **2** (data not shown). The heat instability of **1** can be rationalized by the opening of its five-membered ring to produce **3**, which then undergoes a retro-Michael addition reaction to produce free FAD.

Crystal Structure of PCPA-Modified LSD1. To further understand the mechanism of LSD1 inactivation by PCPA, we determined the crystal structure of PCPA-inactivated LSD1−CoREST using diffraction data to a resolution of 2.75 Å (Figure 4). Although the moderate resolution of the electron density did not allow us to unambiguously assign the chemical structure of the FAD−PCPA adduct, one of the diastereomers of compound **1** fitted very well within this density (Figure 4). In particular, there was strong electron density connecting to N(5) and C(4a) of FAD, indicating that both atoms were modified. In addition, the electron density belonging to the phenyl group could be easily located. On the other hand, compound **4** did not fit with this electron density. Thus, these structural data, along with the mass spectrometry and UV/vis spectroscopy data described above, strongly suggest that compound **1** is the major FAD−PCPA adduct formed during inactivation of LSD1. There are three chiral carbons at C(4a), C(11), and C(13) in **1**. Our structure provides a straightforward rationale for the enatioselectivity at these chiral centers. For example, only one face of FAD in LSD1 is solvent-accessible, and attack of FAD by PCPA from this face generates the observed chirality at C(4a).

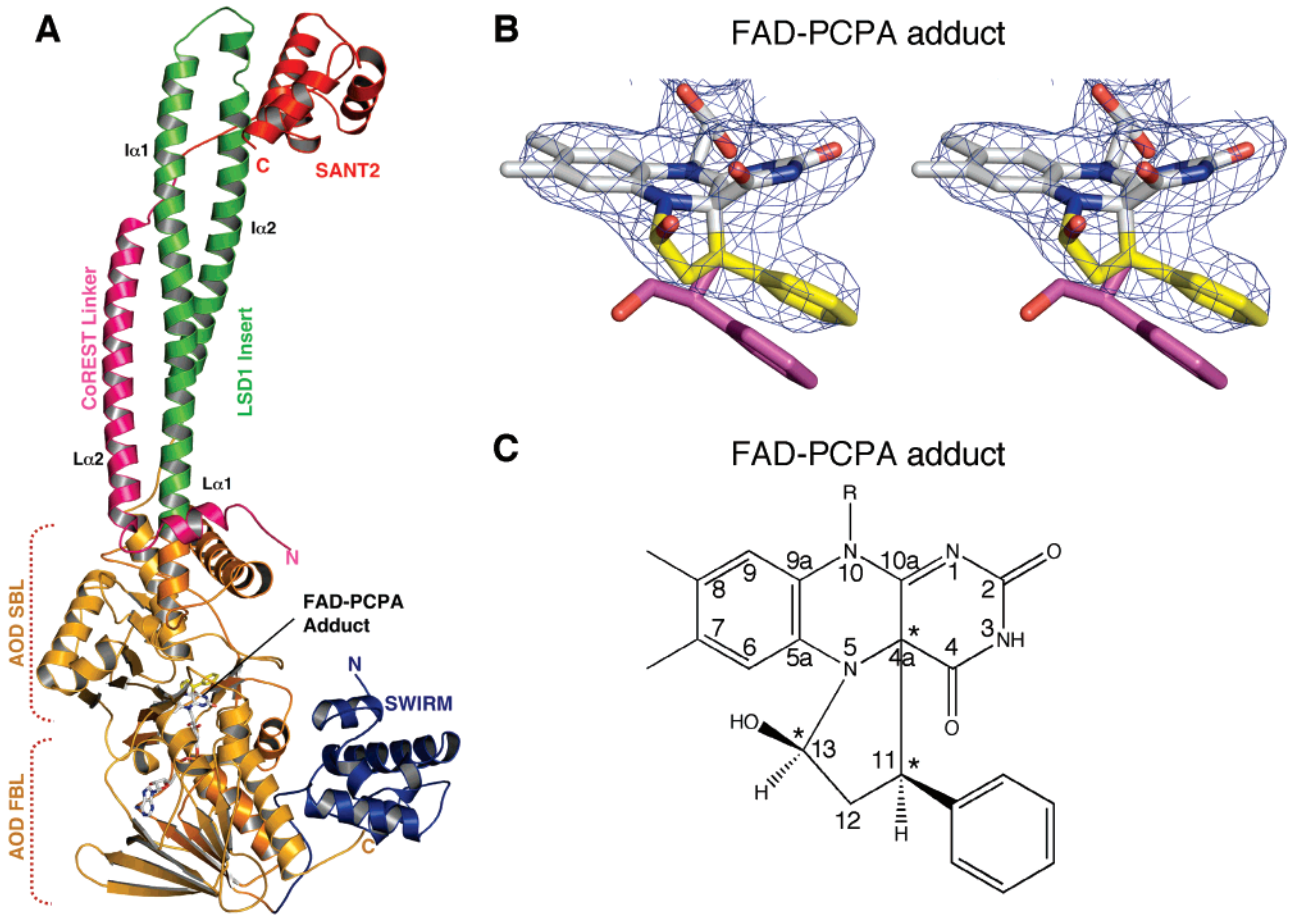

FIGURE 4: Structure of PCPA-modified LSD1−CoREST. (A) Ribbon diagram of LSD1−CoREST with the FAD−PCPA adduct shown in sticks. The SWIRM domain, the amine oxidase domain (AOD), and the insert in the AOD domain of LSD1 are colored in blue, gold, and green, respectively. The SANT2 domain of CoREST is colored in red, while the linker between its SANT1 and SANT2 domains is colored in magenta. (B) Stereoview of the FAD−PCPA adduct shown as a stick model overlaid with the $2F_o-F_c$ σ_A-weighted electron-density map contoured at 1.5σ. Compound **4** is shown as a purple stick model to illustrate that it does not fit the electron density. (C) Chemical structure of the FAD−PCPA adduct that is consistent with the electron density shown in B. The chiral carbon centers are indicated by asterisks. R = ribulose−ADP.

Reversal of the C(11) chirality will create steric clashes between the phenyl group of PCPA and Y761 of LSD1. The hydroxyl group at C(13) forms a hydrogen bond with the C(4) carbonyl oxygen of FAD in **1**, thus explaining the enantioselectivity at C(13).

Interactions between PCPA and the Active-Site Residues of LSD1. The backbone root-mean-square deviation (rmsd) between unmodified and PCPA-modified LSD1−CoREST is 0.42 Å, indicating that PCPA does not induce significant structural changes in LSD1−CoREST. Consistent with its low potency in inhibiting LSD1, there are few interactions between the remnants of PCPA and the active-site residues of LSD1 (Figure 5A). Interestingly, the phenyl ring of the FAD−PCPA adduct is located in a hydrophobic pocket formed by V333, H564, T335, T810, A809, and Y761 (Figure 5B). This phenyl group makes weak van der Waals contacts with the methyl groups of T335 and T810 and fails to make extensive contacts with other surrounding hydrophobic residues, including Y761, V333, and H564. Thus, our structure suggests that one could design PCPA analogues with hydrophobic substitutions on the phenyl ring, which might more fully engage these surrounding hydrophobic residues and inhibit LSD1 with higher potency.

Structure Comparison with PCPA-Modified MAO B. As mentioned above, compound **4** is the adduct formed during inactivation of MAO B by PCPA (*30*). Our results are more consistent with compound **1** being the major FAD−PCPA adduct during LSD1 inactivation, analogous to the inhibition of MSOX by CPG (*31*). How can the same inhibitor form different covalent adducts with the FAD molecules in two homologous enzymes that use similar mechanisms for catalysis? In MAO B, Y389 and Y435 form a so-called "aromatic sandwich" that lies directly above the isoalloxazine ring of FAD and positions substrates for catalysis (Figure 5C). Formation of **1** would lead to a steric clash between the phenyl group of the adduct and Y435 in MAO B. In contrast, the formation of **4** avoids this steric clash and places the phenyl group in a hydrophobic pocket formed by residues Y435, Y389, Q206, Y60, and F343. Thus, the geometry of the active site of MAO B prohibits the formation of **1**, thus favoring the formation of **4**. In the case of LSD1, Y435 is replaced by a much smaller residue, T810, which makes space for the phenyl ring in **1**. On the other hand, the formation of **4** in LSD1 would result in a steric clash between the phenyl ring of PCPA and F538 and Y761 of LSD1. Thus, despite the similarities in their catalytic mechanisms, the differences in the active-site residues of LSD1 and MAO B lead to the formation of distinct FAD−PCPA covalent adducts.

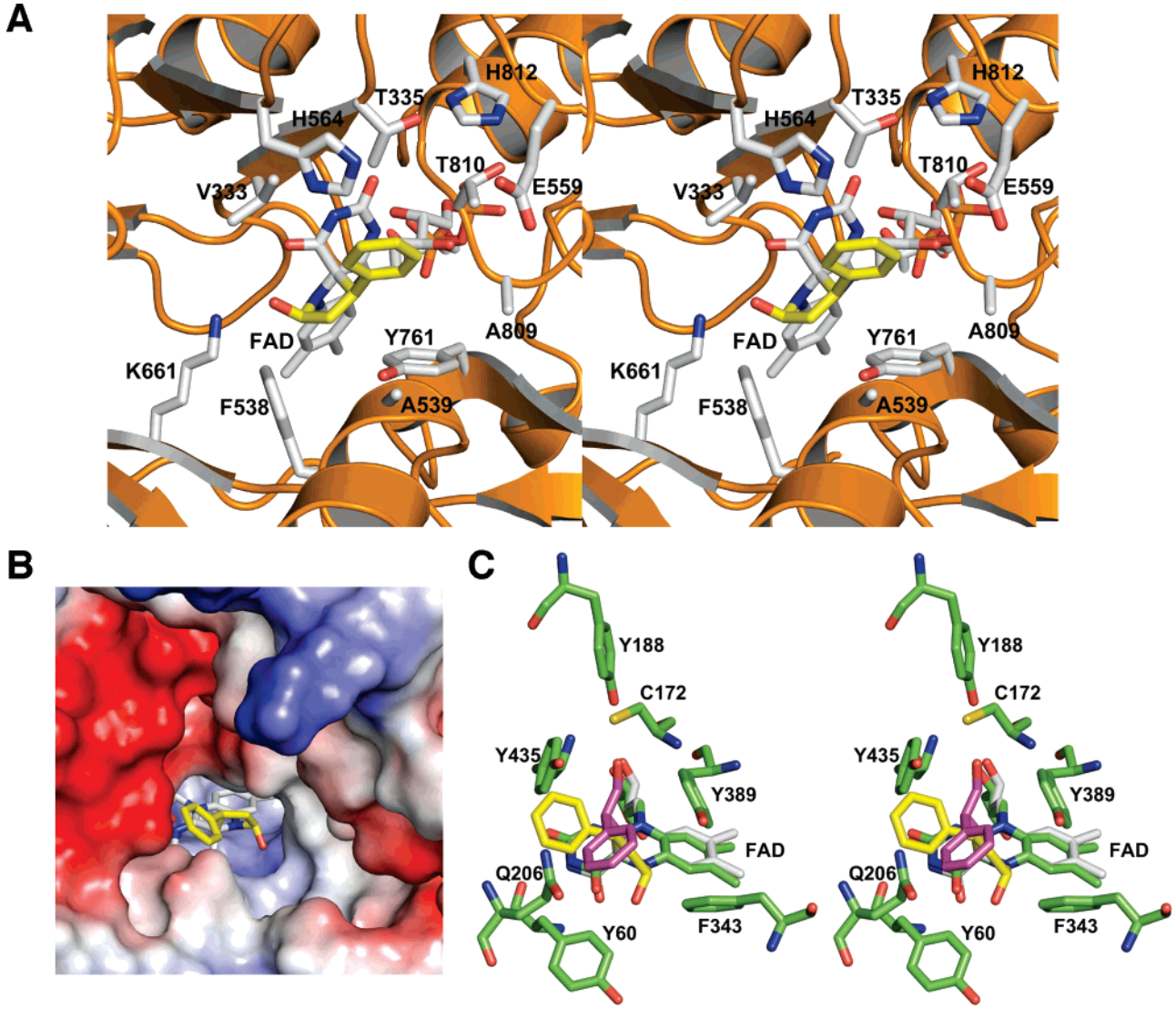

FIGURE 5: Active site of LSD1. (A) Stereoview of the FAD−PCPA adduct and its surrounding residues at the active site of LSD1. The LSD1 residues and FAD are shown as stick models with their carbon, nitrogen, and oxygen atoms colored gray, blue, and red, respectively. The carbon and oxygen atoms derived from PCPA are colored yellow and red, respectively. (B) Surface diagram of LSD1 with its positive and negative electrostatic potentials colored blue and red, respectively. The FAD−PCPA adduct is shown in a stick model with the same color scheme as in A. (C) Stereoview of the MAO B active site with its FAD−PCPA adduct (green, with the atoms derived from PCPA shown in purple) superimposed with the FAD−PCPA adduct in LSD1 (gray, with the atoms derived from PCPA shown in yellow).

CONCLUSIONS

Because LSD1 and MAO share sequence and structural similarity and use similar chemical mechanisms for catalysis, certain inhibitors of MAOs also inhibit LSD1 efficiently. We have further characterized inhibition of LSD1 by the MAO inhibitor, PCPA (tranylcypromine), a clinically used antidepressant. Our biochemical and structural studies are consistent with the formation of a covalent adduct between PCPA and the FAD cofactor in LSD1. Because PCPA is a mechanism-based inactivator of LSD1, our results further support a single-electron-transfer mechanism for lysine demethylation by LSD1, as previously proposed for MAO (*32*). Interestingly, despite the similarity between LSD1 and MAO in their catalytic mechanisms, inactivation of LSD1 and MAO B by PCPA results in the formation of distinct covalent FAD−PCPA adducts. Furthermore, the phenyl group of the FAD−PCPA adduct in LSD1 is located in a large hydrophobic pocket and does not form extensive contacts with surrounding residues, suggesting that PCPA analogues with hydrophobic substitutions on the phenyl ring might be more potent inhibitors of LSD1. Furthermore, the structural characteristics of the LSD1 active site can be exploited to create LSD1 inhibitors with high specificity, thus avoiding potential side effects associated with inhibiting structurally similar enzymes, such as MAOs. Our structure serves as a valuable scaffold for the design of such PCPA analogues. LSD1 and HDACs are frequently found in the same transcriptional corepressor complexes, and they collaborate to establish epigenetic marks that silence transcription. Inhibitors of HDACs are promising new anticancer drugs. Therefore, inhibitors of LSD1 may also have therapeutic potential in treating human cancers, either on their own or in combination with HDAC inhibitors.

ACKNOWLEDGMENT

We thank Na Wang for help with crystallization. We also thank members of the Yu laboratory for helpful discussions. Results shown in this paper are derived from work performed

at Argonne National Laboratory, Structural Biology Center at the Advanced Photon Source. Argonne is operated by University of Chicago Argonne, LLC, for the U.S. Department of Energy, Office of Biological and Environmental Research, under contract DE-AC02-06CH11357.

REFERENCES

1. Jenuwein, T., and Allis, C. D. (2001) Translating the histone code, *Science 293*, 1074−1080.
2. Schreiber, S. L., and Bernstein, B. E. (2002) Signaling network model of chromatin, *Cell 111*, 771−778.
3. Martin, C., and Zhang, Y. (2005) The diverse functions of histone lysine methylation, *Nat. Rev. Mol. Cell Biol. 6*, 838−849.
4. Ruthenburg, A. J., Allis, C. D., and Wysocka, J. (2007) Methylation of lysine 4 on histone H3: Intricacy of writing and reading a single epigenetic mark, *Mol. Cell 25*, 15−30.
5. Shi, Y., and Whetstine, J. R. (2007) Dynamic regulation of histone lysine methylation by demethylases, *Mol. Cell 25*, 1−14.
6. Shi, Y., Lan, F., Matson, C., Mulligan, P., Whetstine, J. R., Cole, P. A., Casero, R. A., and Shi, Y. (2004) Histone demethylation mediated by the nuclear amine oxidase homolog LSD1, *Cell 119*, 941−953.
7. Forneris, F., Binda, C., Vanoni, M. A., Mattevi, A., and Battaglioli, E. (2005) Histone demethylation catalysed by LSD1 is a flavin-dependent oxidative process, *FEBS Lett. 579*, 2203−2207.
8. Hakimi, M. A., Dong, Y., Lane, W. S., Speicher, D. W., and Shiekhattar, R. (2003) A candidate X-linked mental retardation gene is a component of a new family of histone deacetylase-containing complexes, *J. Biol. Chem. 278*, 7234−7239.
9. Humphrey, G. W., Wang, Y., Russanova, V. R., Hirai, T., Qin, J., Nakatani, Y., and Howard, B. H. (2001) Stable histone deacetylase complexes distinguished by the presence of SANT domain proteins CoREST/kiaa0071 and Mta-L1, *J. Biol. Chem. 276*, 6817−6824.
10. Shi, Y., Sawada, J., Sui, G., Affar, E. B., Whetstine, J. R., Lan, F., Ogawa, H., Luke, M. P., Nakatani, Y., and Shi, Y. (2003) Coordinated histone modifications mediated by a CtBP co-repressor complex, *Nature 422*, 735−738.
11. You, A., Tong, J. K., Grozinger, C. M., and Schreiber, S. L. (2001) CoREST is an integral component of the CoREST−human histone deacetylase complex, *Proc. Natl. Acad. Sci. U.S.A. 98*, 1454−1458.
12. Shi, Y. J., Matson, C., Lan, F., Iwase, S., Baba, T., and Shi, Y. (2005) Regulation of LSD1 histone demethylase activity by its associated factors, *Mol. Cell 19*, 857−864.
13. Lee, M. G., Wynder, C., Cooch, N., and Shiekhattar, R. (2005) An essential role for CoREST in nucleosomal histone 3 lysine 4 demethylation, *Nature 437*, 432−435.
14. Yang, M., Gocke, C. B., Luo, X., Borek, D., Tomchick, D. R., Machius, M., Otwinowski, Z., and Yu, H. (2006) Structural basis for CoREST-dependent demethylation of nucleosomes by the human LSD1 histone demethylase, *Mol. Cell 23*, 377−387.
15. Jones, P. A., and Baylin, S. B. (2007) The epigenomics of cancer, *Cell 128*, 683−692.
16. Minucci, S., and Pelicci, P. G. (2006) Histone deacetylase inhibitors and the promise of epigenetic (and more) treatments for cancer, *Nat. Rev. Cancer 6*, 38−51.
17. Lee, M. G., Wynder, C., Bochar, D. A., Hakimi, M. A., Cooch, N., and Shiekhattar, R. (2006) Functional interplay between histone demethylase and deacetylase enzymes, *Mol. Cell. Biol. 26*, 6395−6402.
18. Shih, J. C., Chen, K., and Ridd, M. J. (1999) Monoamine oxidase: From genes to behavior, *Annu. Rev. Neurosci. 22*, 197−217.
19. Culhane, J. C., Szewczuk, L. M., Liu, X., Da, G., Marmorstein, R., and Cole, P. A. (2006) A mechanism-based inactivator for histone demethylase LSD1, *J. Am. Chem. Soc. 128*, 4536−4537.
20. Szewczuk, L. M., Culhane, J. C., Yang, M., Majumdar, A., Yu, H., and Cole, P. A. (2007) Mechanistic analysis of a suicide inactivator of histone demethylase LSD1, *Biochemistry*, *46*, 6892−6902.
21. Lee, M. G., Wynder, C., Schmidt, D. M., McCafferty, D. G., and Shiekhattar, R. (2006) Histone H3 lysine 4 demethylation is a target of nonselective antidepressive medications, *Chem. Biol. 13*, 563−567.
22. Schmidt, D. M., and McCafferty, D. G. (2007) *trans*-2-Phenylcyclopropylamine is a mechanism-based inactivator of the histone demethylase LSD1, *Biochemistry 46*, 4408−4416.
23. Otwinowski, Z., and Minor, W. (1997) Processing X-ray diffraction data collected in oscillation mode, *Methods Enzymol. 276*, 307−326.
24. Murshudov, G. N., Vagin, A. A., and Dodson, E. J. (1997) Refinement of macromolecular structures by the maximum-likelihood method, *Acta Crystallogr., Sect. D: Biol. Crystallogr. 53*, 240−255.
25. Consortium, T. C. (1994) The CCP4 suite: Programs for protein crystallography, *Acta Crystallogr., Sect. D: Biol. Crystallogr. 50*, 760−763.
26. Emsley, P., and Cowtan, K. (2004) Coot: Model-building tools for molecular graphics, *Acta Crystallogr., Sect. D: Biol. Crystallogr. 60*, 2126−2132.
27. Forneris, F., Binda, C., Vanoni, M. A., Battaglioli, E., and Mattevi, A. (2005) Human histone demethylase LSD1 reads the histone code, *J. Biol. Chem. 280*, 41360−41365.
28. Copeland, R. A. (2000) *Enzymes: A Practical Introduction to Structure, Mechanism, and Data Analysis*, 2nd ed., Wiley-VCH, New York.
29. Kitz, R., and Wilson, I. B. (1962) Esters of methanesulfonic acid as irreversible inhibitors of acetylcholinesterase, *J. Biol. Chem. 237*, 3245−3249.
30. Binda, C., Li, M., Hubalek, F., Restelli, N., Edmondson, D. E., and Mattevi, A. (2003) Insights into the mode of inhibition of human mitochondrial monoamine oxidase B from high-resolution crystal structures, *Proc. Natl. Acad. Sci. U.S.A. 100*, 9750−9755.
31. Chen, Z. W., Zhao, G., Martinovic, S., Jorns, M. S., and Mathews, F. S. (2005) Structure of the sodium borohydride-reduced *N*-(cyclopropyl)glycine adduct of the flavoenzyme monomeric sarcosine oxidase, *Biochemistry 44*, 15444−15450.
32. Silverman, R. B. (1995) Radical ideas about monoamine oxidase, *Acc. Chem. Res. 28*, 335−342.

BI700664Y